

# Tweezers with a twist

Miles Padgett\* and Richard Bowman

**The fact that light carries both linear and angular momentum is well-known to physicists. One application of the linear momentum of light is for optical tweezers, in which the refraction of a laser beam through a particle provides a reaction force that draws the particle towards the centre of the beam. The angular momentum of light can also be transferred to particles, causing them to spin. In fact, the angular momentum of light has two components that act through different mechanisms on various types of particle. This Review covers the creation of such beams and how their unusual intensity, polarization and phase structure has been put to use in the field of optical manipulation.**

Almost two decades ago, Allen *et al.*<sup>1</sup> introduced the optics community to the concept that light beams could carry an angular momentum additional and independent of the photon spin. Three years later, Rubinsztein-Dunlop and co-workers<sup>2</sup> used one of these beams to spin a microscopic particle held in optical tweezers, through a technique that was subsequently referred to as ‘optical spanners’<sup>3</sup>. In 1909, Poynting reasoned that a circularly polarized light beam of angular frequency  $\omega$  should carry a small amount of angular momentum, such that the ratio between its angular momentum and energy is  $1/\omega$  (ref. 4). Although Poynting’s calculation was purely classical, it is today interpreted in terms of photons by considering that a photon of energy  $\hbar\omega$  has an angular momentum of  $\sigma\hbar$ , where  $\sigma = 1$  or  $-1$  for left- and right-handed circular polarizations, respectively. Poynting himself did not have much hope that observing an optically induced torque on a mechanical object was possible. However, in 1936 Beth showed that using a birefringent waveplate to convert between left- and right-handed circular polarizations introduces angular momentum to the light, which acts as a counter-torque on the waveplate. Beth observed this torque by suspending a waveplate using thin fibre and noting the induced rotations<sup>5</sup>.

The angular momentum associated with circular polarization is a manifestation of photon spin. However, it has been known from the early days of electromagnetic theory that light can carry additional angular momentum associated with its spatial distribution<sup>6</sup>. For example, whereas an atomic dipole transition is naturally associated with an angular momentum of  $\hbar$ , multipole transitions require higher changes in angular momentum and therefore it must be possible for a single photon to carry multiple units of  $\hbar$ . Simplistically, multiplying a linear momentum by a radius vector gives an angular momentum. Consequently, any skewed ray within an optical system can be considered as having an angular momentum about the beam axis. Such rays are the basis of the orbital angular momentum (OAM) of light.

## Orbital angular momentum in laboratory light beams

The breakthrough of the 1992 paper by Allen *et al.* was to recognize that laser beams carrying defined amounts of OAM could be produced in the laboratory, and that such beams would be perfectly described by the Laguerre–Gaussian mode set<sup>1</sup>. Laguerre–Gaussian modes have an annular intensity structure and incorporate an azimuthal phase structure of  $e^{i\ell\phi}$ , where  $\phi$  is the azimuthal angle and  $\ell$  is the mode index, which can take any integer value. This azimuthal phase term corresponds to a helical phase surface (shown in Fig. 1), meaning that the Poynting vector has a non-zero azimuthal component at every radial position  $r$  in the beam. The associated momentum flow per photon is given as  $p_\phi = (h/\lambda) \times (\ell\lambda/2\pi r)$ , where  $p_\phi$  is



**Figure 1 | Light beams can carry both OAM and spin angular momentum.**

Here, OAM is represented by helical phasefronts, and spin angular momentum is represented by a polarization vector, which rotates as the beam propagates.

the photon momentum and  $\lambda$  is the wavelength of the light. When multiplied by the radius vector this azimuthal component of the linear momentum gives an angular momentum about the beam axis of  $\ell\hbar$  (ref. 7).

Allen *et al.* used a clever combination of cylindrical lenses to near-perfectly transform the high-order Hermite–Gaussian mode from a conventional laser into a single Laguerre–Gaussian mode<sup>8</sup>. At around the same time, however, parallel studies using simple diffractive optical elements made of diffraction gratings with an  $\ell$ -fork dislocation on the beam axis were producing similar beams<sup>9,10</sup>. When illuminated with a fundamental Gaussian beam, the first-order diffracted beam produced by such an element has an  $e^{i\phi}$  phase structure and an intensity cross-section in which most of the beam energy is contained within a single bright ring. The resulting beam is a close approximation to a Laguerre–Gaussian mode. Strictly speaking, the beam is a superposition of many Laguerre–Gaussian modes, all with the same  $\ell$  but differing radial mode indices. The intensity cross-section of the beam contains additional annular lobes of low intensity at different radii to the main ring. If necessary, these lobes can be suppressed by slight modifications to the diffractive optic design<sup>11</sup>. The original interest in these diffractively produced beams was not their angular momentum (to which no reference was made), but instead as examples of optical phase-singularities<sup>12,13</sup> and optical vortices<sup>14</sup>. Photographic methods, which are often used to produce diffractive optical components, are now capable of producing such forked gratings on a pixellated, liquid-crystal spatial light modulator (SLM). SLMs can be addressed by a computer to implement almost any diffractive element of choice — the fork diffraction

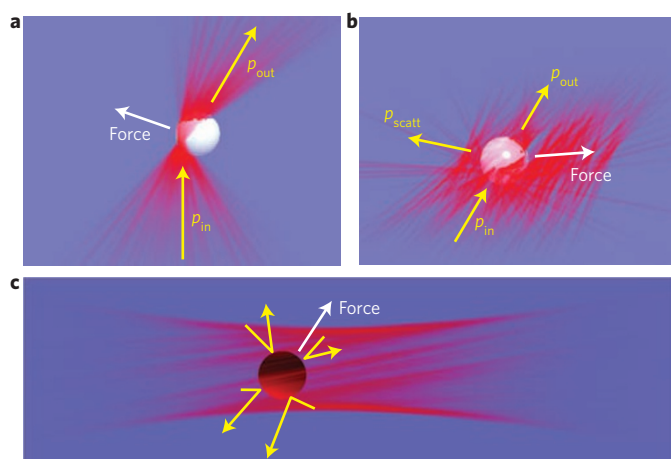


**Figure 2 | Several different force mechanisms are involved in optical trapping.** **a**, The ‘gradient force’, in which a refractive particle moves towards the brightest point of the beam.  $p_{in}$  is the momentum of the incident light and  $p_{out}$  is the momentum of the refracted light. **b**, Reflected or otherwise scattered light (with momentum  $p_{scatt}$ ) pushes the particle in the direction of the Poynting vector, which is known as the ‘scattering force’. **c**, An absorbing particle can be locally heated, creating a thermal gradient across its surface. Molecules rebound faster off the hot side than the cold side, resulting in a force that can levitate, trap and transport particles.

grating being just one example. These devices do however require considerable care to produce aberration-free beams<sup>15,16</sup>.

### Optical tweezers

From the 1970s onwards, Ashkin and co-workers pioneered the application of laser beams to the manipulation of microscopic and atomic systems. In fact, it was the work of Ashkin *et al.* in 1986<sup>17</sup> that initiated the field of optical tweezers, from which most of the work in this Focus Issue derives. In normal optical tweezers, a tightly focused Gaussian beam creates a bright focus at which the electric field is a maximum. Any dielectric (that is, transparent) particle experiences a force that moves it towards the beam focus, as shown in Fig. 2. Combined with additional forces due to light scattering and gravity, the resulting ‘gradient force’ provides a stable trap position close to the focal point of the beam. Dynamical stability is ensured because optical tweezers mainly operate on particles suspended in a fluid medium, the viscosity of which damps any oscillations. However, although optical tweezers work well for most transparent particles, absorbing particles experience a much higher scattering force that often prevents the formation of a stable trap. In addition, thermal heating can create unwanted forces that may allow particles to escape.

### Optical spanners

In 1995, Rubinsztien-Dunlop and co-workers produced an OAM-carrying annular beam using a forked diffraction grating and then implemented this beam in an optical tweezer set-up<sup>18</sup>. They showed that absorbing particles could be held at the dark centre of the beam and confined against the microscope slide. Even more excitingly, they showed that the absorption of light and associated OAM led to an optically induced rotation of the particle<sup>2</sup>. These experiments were the first to confirm that the OAM of light could be coupled to a mechanical system.

Although this work demonstrated the mechanical reality of OAM, the torque associated with the rotating particles proved difficult to calibrate. Inferred measurement (rather than direct measurement) was made by comparing the torque associated with OAM to that

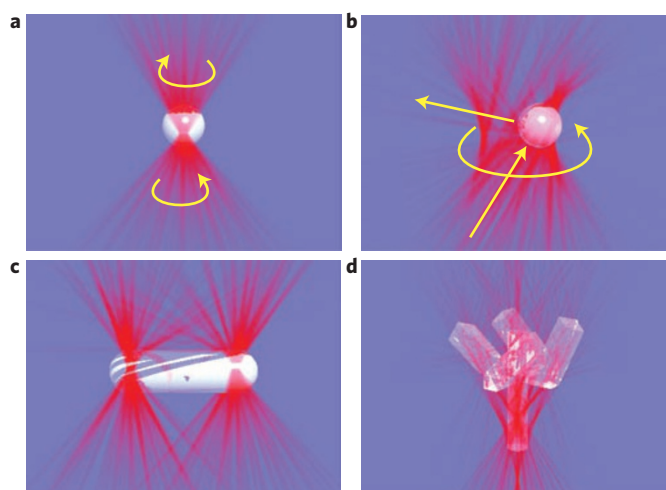


**Figure 3 | Different methods of applying optical torque.** **a**, Using a birefringent particle to change a beam’s polarization state and therefore its spin angular momentum. **b**, Using the scattering force to circulate a small particle around the bright ring of a Laguerre–Gaussian beam. **c**, Using an asymmetric beam shape to align an asymmetric object. **d**, Using a shaped object to scatter light into an OAM-containing mode.

produced by the photon’s spin component. In terms of absorption, the transfer of orbital or spin angular momentum should be equivalent. Later experiments exploited circularly polarized Laguerre–Gaussian modes, which allow the orbital and spin components of angular momentum to be added or subtracted. Friese *et al.* showed that a beam with  $l = 3$  and  $\sigma = 1$  or  $-1$  has a total angular momentum of  $2\hbar$  or  $4\hbar$  per photon, respectively, as well as a factor of two difference in rotation speed<sup>19</sup>. In contrast, Simpson *et al.* showed that a beam of  $l = 1$  and  $\sigma = 1$  or  $-1$  has a total angular momentum of 0 or  $2\hbar$  per photon, respectively, allowing the particle rotation to be stopped completely<sup>3</sup>. In the work of Simpson *et al.*, the particles could be trapped in three dimensions because they were only partially absorbing.

Optical absorption is a universal way of converting between spin angular momentum and OAM, but it is not the only possible mechanism. For OAM, any process that transforms the laser mode to or from a helically phased beam must transfer OAM. Similarly, any optical process that transforms the polarization state will transfer spin angular momentum. Some mechanisms for transferring angular momentum are illustrated in Fig. 3. In 1998, a beautiful experiment by Rubinsztien-Dunlop and co-workers<sup>20</sup> used calcite particles as tiny waveplates to perform the microscopic equivalent of Beth’s original experiment. Whereas Beth suspended his waveplate from a fibre, Rubinsztien-Dunlop and co-workers held their microscopic waveplate in an optical trap, thus providing a rotation frequency of many hertz.

These experiments collectively demonstrated not only that the optical angular momentum could be transferred to small particles, but also that its characterization in terms of multiples of  $\hbar$  per photon was appropriate. Perhaps more importantly, the demonstrated rotation rates of many hertz suggested that such techniques could form the basis of optically driven sensors and machines for microfluidic environments.

### Rotational control with shaped beams

Optically induced rotation within optical tweezers actually predates any recognition of OAM. An elongated object in a non-circular beam will orient such as to maximize its overlap with the high-intensity region of the light. In very early work, Ashkin observed that

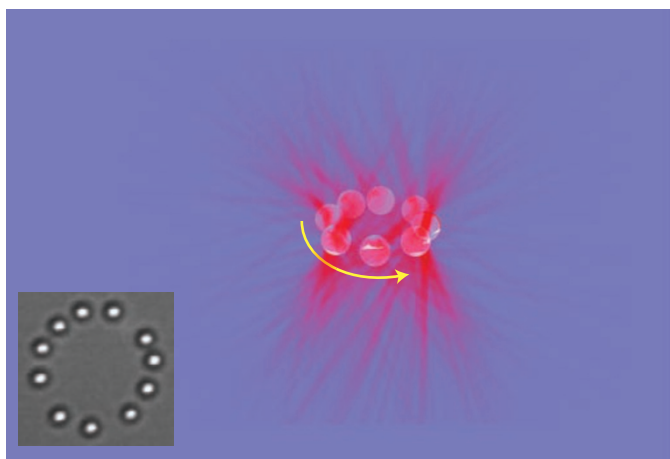


**Figure 4 | 1- $\mu\text{m}$ -diameter beads circulate when held in an optical vortex.**

A micrograph of the experiment is shown in the inset. The scattering force drives particles around the ring of a high- $I$  beam, during which they experience random forces from Brownian motion and exhibit interesting dynamics as a consequence of hydrodynamic interactions.

rod-like bacteria would align themselves along the trapping axis of a laser beam<sup>21</sup>. Sato *et al.* subsequently used the rectangular cross-section of a high-order Hermite–Gaussian mode to trap and orientate a red blood cell<sup>22</sup>, whereby rotation of the mode cross-section resulted in a corresponding rotation of the cell. Other approaches for forming non-cylindrical beams have included annular interference patterns<sup>23,24</sup>, a rectangular aperture in the beam path<sup>25</sup> and the use of multimode fibre<sup>26</sup>. Objects can also be oriented using two point-traps, and by defocusing one trap it is possible to orient objects in three dimensions<sup>27</sup>. Linear polarization breaks the circular symmetry of the trapping beam, and this has been used to align birefringent objects with the polarization vector<sup>28,29</sup>.

Rotation can also be achieved by shaping the particle itself. Designing the particle such that some of the light is scattered in the azimuthal direction allows it to impart angular momentum to the scattered light. The angular momentum of the scattered light gives a reaction torque on the rotor and a corresponding rotation about the optical axis. Higurashi *et al.* used reactive ion-beam etching to create miniature rotors that could be driven at rates of around 1 Hz (refs 30,31). In a similar configuration (using a high-numerical-aperture microscope for optical trapping), Galajda and Ormos trapped shaped objects fabricated through two-photon polymerization<sup>32,33</sup>. Since then a number of groups have used this approach to make sophisticated rotors and mode-converters for transforming the mode of the trapping beam — a clear route to making and driving micromachines within optical tweezers<sup>34</sup>. The same technique has also been used to achieve rotation about an axis perpendicular to the beam axis<sup>35</sup>.

Helically phased beams all have an annular intensity profile that is independent of any angular momentum properties. Indeed, it was this on-axis intensity minimum that allowed absorbing particles to be confined in the original rotation work of Rubinsztajn–Dunlop and co-workers<sup>2</sup>. Since then, the annular nature of Laguerre–Gaussian beams has, for example, been used to confine metal nanoparticles in situations when residual scattering of the OAM has set the particles into rotation<sup>36</sup>. By blue-detuning the optical trap, two or more particles can be confined in the same beam, yet do not attach to each other because of plasmon resonances.

### Trapping with annular beams

Beams carrying OAM about the beam axis can be focused to shapes other than that of a single diffraction-limited spot. Most OAM-

carrying beams used in optical trapping form an annular intensity distribution in the focal plane. The use of annular beams for optical trapping was first suggested by Ashkin, who recognized that trapping in the axial direction could be enhanced if the on-axis rays were removed from the beam<sup>37</sup>. Ashkin envisaged using a beam-stop to create the annulus, although subsequent work achieved this using Laguerre–Gaussian beams<sup>38,39</sup>. Thanks to the scattering force, a Laguerre–Gaussian beam can confine absorbing particles at the centre of its annulus. However, such beams are also capable of trapping other particles. If the particle is transparent but has a lower refractive index than the surrounding fluid, the gradient force gives rise to a stable trap on the beam axis. In normal optical tweezers this reversal of the refractive index contrast would result in the particle being expelled from the beam. Gahagan and Swartzlander showed that a trap comprising a low-refractive-index particle held in a Laguerre–Gaussian beam the trap is stable in three dimensions<sup>40</sup>. Such techniques have been applied to the manipulation and filtration of hollow glass spheres, with the potential for targeted drug delivery<sup>41</sup>. Another application of trapping low-refractive-index spheres is the fusion of aqueous droplets within a higher-refractive-index oil medium, creating the potential for chemistry on a femtolitre scale<sup>42</sup>.

### Spinning and orbiting in optical tweezers

Early work involved particles that were typically large compared with the beam size, thus confining them at (or near to) the beam axis. Under such a geometry, transferring either spin or OAM causes the particle to spin around its axis. In 2002, Padgett and co-workers used a large Laguerre–Gaussian beam to trap small particles around the bright ring, as shown in Fig. 4<sup>43</sup>. Silica particles were confined in the bright annulus by the gradient force and made to rotate by the scattering force. The beam was circularly polarized to carry spin angular momentum as well as OAM; birefringent calcite particles were trapped in the beam and observed to spin about their own axes. By choosing particles that were both birefringent and optically scattering, simultaneous spinning and orbiting of the particles was observed<sup>44</sup>. The radius at which the particles orbit varies with the wavelength (and hence with the OAM) of the beam<sup>45</sup>. When such annular beams are large, the axial trapping of the system is weak and it is often necessary to axially restrain the particles in other ways, for example within a thin sample cell or at the fluid–air interface<sup>46</sup>.

Although OAM is usually associated with a laser mode, which is typically of a single wavelength, monochromatic light is not a fundamental requirement. Just as white light can be circularly polarized, it can also be helically phased<sup>47</sup>. However, a pure OAM state requires spatial coherence, whereas a pure polarization state does not. Laser beams can also be white-light in nature and converted to have pure helical phasefronts using a forked diffraction grating that is then re-imaged onto a second component to correct for angular dispersion<sup>48,49</sup>. Using similar white-light vortex beams it is possible to set particles into rotation around the beam axis<sup>50</sup>. It is also possible to produce annular beams with fractional values of  $l$ , which are not pure OAM modes. Although particles have been shown to circulate in such beams, their intensity structure is not circularly symmetric, which modifies the circulation for some beams and/or particle sizes. This size dependence of the circulation suggests applications in particle sorting and selection<sup>51</sup>.

One interesting feature of all such investigations is that they highlight how different transfer mechanisms apply to spin angular momentum and OAM. With respect to OAM transfer, they highlight how angular momentum arises solely from the azimuthal component of optical linear momentum acting on a radius vector. One sees immediately that the maximum angular momentum transfer to any object cannot exceed the linear momentum of the light multiplied by the radius of the object itself (multiplied by two in the case of reflection)<sup>52</sup>.



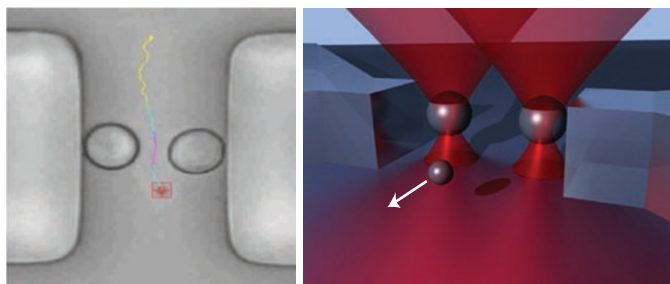


**Figure 5 | A microfluidic pump can be created using two birefringent particles.** The particles counter-rotate because they are in circularly polarized traps with opposite handedness, thus causing a fluid flow in the region between them.

### Interactive beam shaping

As mentioned previously, the use of diffractive optics for beam shaping in optical tweezers has been transformed by the commercial availability of computer-controlled SLMs. SLMs were first used in optical tweezers in the late 1990s<sup>53,54</sup>. In particular, Tiziani, Haist and co-workers showed how simple algorithms could create multiple traps within optical tweezers, and that these traps could be shaped into annular beams with helical phasefronts<sup>55</sup>. However, the wider appeal of using SLMs in tweezers was triggered by Grier and co-workers, who demonstrated the flexibility and ease at which this technique — coined ‘holographic optical tweezers’ — could be implemented<sup>56,57</sup>. They used this technique to undertake a number of studies, including one that demonstrated how a non-uniform azimuthal phase gradient could transform the ring into clover-leaf-type patterns, around which the confined particles would circulate<sup>58</sup>. The precise shape and degree of symmetry of a helically phased beam is highly dependent on any aberrations in the optical system. For example, astigmatism causes the annular intensity distribution to become elliptical. This effect has been applied by Ritsch-Marte and co-workers to the measurement and subsequent correction of aberrations in optical systems, including optical tweezers, and particularly to the correction of aberrations introduced by the SLM itself<sup>16</sup>. SLMs have also been used to modify the polarization state of light beams, allowing multiple particles to be trapped and independently rotated<sup>59,60</sup>.

Grier and co-workers have used OAM-carrying beams as one beam type within their wider studies of hydrodynamic interactions and Brownian motion. An annular ring approximates to a 1D periodic line in which particles are confined but driven in a single direction by the scattering force. If several particles are trapped in the same ring then they become weakly coupled by the slipstreaming of one particle within the fluid flow created by another<sup>61</sup>. When particles are trapped in concentric rings, the motion of particle creates a fluid flow that exerts a drag on all those around it<sup>62</sup>. Deliberately interfering the vortex beam with its own mirror image gives rise to an azimuthal intensity modulation that creates a periodic potential within the 1D periodic system, against which various predictions relating to particle mobility can be tested<sup>63</sup>. In related work, particles circulating around the annulus of OAM-carrying beams have been used to create fluid flow and hence form an optically driven pump<sup>64</sup>.

### Spinning particles as tools

The viscosity of the fluid surrounding a trapped particle in conventional optical tweezers can be probed through residual Brownian motion<sup>65</sup>, but measurements using driven rotational motion offer a simpler way of achieving the same goal. Rubinstein-Dunlop and co-workers demonstrated that their technique of transferring spin angular momentum to microscopic calcite particles could be used to measure fluid viscosity<sup>66</sup>. Rather than relying on natural calcite

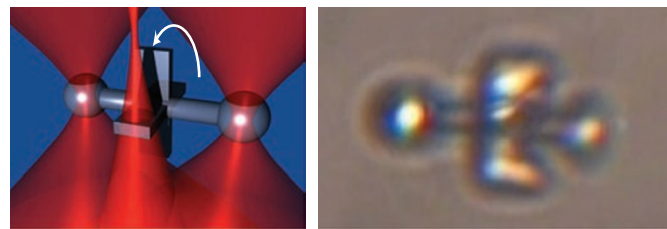


**Figure 6 | A microfabricated paddle-wheel is driven by the scattering force from a laser beam.** Two optical traps hold the shaft in place, while a third beam pushes the blades round. None of the beams have spin angular momentum or OAM in isolation, but light scattered off the blades imparts angular momentum about the axis of the shaft. Photomicrograph (right) courtesy of Asavei *et al.*<sup>77</sup>.

crystals, which are often irregular in shape, they developed a chemical technique to grow perfectly spherical birefringent particles of vaterite<sup>67,68</sup>. When trapped in a circularly polarized beam, vaterite particles spin at frequencies of many hertz with a speed that is proportional to the trapping power and inversely proportional to the viscosity of the surrounding fluid. The spherical nature of the particles means that their speed is deduced not from video imaging but by monitoring the polarization state of the transmitted light. Loading vaterite particles into a sample allows this tweezers-based technique to probe the viscosity of picolitre fluid volumes<sup>67</sup> such as internal cell environments<sup>69</sup>. One advantage of this rotational approach over linear methods lies in the nature of the hydrodynamic coupling between the particle and the surrounding boundaries. However, assuming a no-slip condition for the fluid in contact with neighbouring boundaries results in a reduced particle mobility, which, if left unaccounted for, causes the viscosity to be over-estimated. Faxen provided a correction to the particle mobility that, for linear motion, scales with the inverse of the distance to the boundary. This reduced particle mobility has a much shorter range in the case of rotational motion, where it scales with the inverse cube of the distance. For practical purposes, correction is unnecessary in the rotational case, provided that the separation between the particle and the boundary exceeds the particle diameter<sup>70</sup>. Counter-rotating spinning vaterite particles have also been held on opposite sides of a microfluidic channel such that the surrounding fluid flow causes a net flow along the channel, hence forming a microfluidic pump that is driven by the spin angular momentum of light<sup>71</sup> (Fig. 5).

### Forces at work in optical tweezers

The optical forces discussed so far have been associated either with the gradient force, which relates to the beam's intensity distribution, or the scattering force, which is directed by the beam's transverse phase gradient. The azimuthal phase gradient of a Laguerre-Gaussian beam and the resulting OAM is just one example of a beam that derives its properties from its phase structure. In general, any intensity cross-section can be created to have a specific phase gradient and hence a determined transverse scattering force<sup>72,73</sup>. Furthermore, one can shape the beam in the axial direction to transport particles in three dimensions by a combination of phase gradient and intensity gradient forces<sup>74–76</sup>. This combination can also be used to impart angular momentum about an axis not parallel to the beam, as demonstrated by Asavei *et al.*<sup>77</sup>. Their experiment used two optical traps to hold a structure, while a third caused it to rotate as a result of the scattering force (Fig. 6).

Optically induced forces are not only limited to scattering and gradient forces. In 1982, Lewittes and Arnold used a thermal effect generated by an annular beam to levitate a slightly absorbing sphere of liquid dye<sup>78</sup>. Holding the absorbing particle in air and illuminating

it from one side generated a differential in surface temperature. Surrounding gas molecules rebounded off the hot side of the particle with velocities greater than those bouncing off the cold side, resulting in a net pressure. This photophoretic force can dominate over the radiation pressure by a ratio that is approximately given by the speed of light divided by the molecular velocity. In 2009, Kivshar and co-workers extended and developed this approach to the trapping of highly absorbing particles in air<sup>79</sup>. Their approach allows large ( $>100\ \mu\text{m}$ ) absorbing particles in air to be trapped and transported over metre ranges along the axis of an annular beam<sup>80</sup>. Quite remarkably, they have also shown that the photophoretic force is so large that particles can even be trapped in the dark voids created when light scatters from a rough surface<sup>81</sup>. Such voids are formed by small optical vortex loops<sup>82</sup> and are the three-dimensional equivalent of the black spots observable in laser speckle patterns.

## Conclusions

It has been twenty years since the realization that OAM could be imparted to a well-behaved laser beam. This knowledge has impacted many branches of optical physics, including imaging<sup>83,84</sup>, nonlinear<sup>85</sup> and quantum optics<sup>86</sup>, information encoding<sup>87,88</sup> and, of course, optical manipulation. In many cases it was the idea of OAM that provided the conceptual leaps in both understanding and application. In other areas it is the general recognition that shaping a light beam applies not only to its intensity cross-section but also to its phase cross-section. Undoubtedly, continuing advances in SLM technology, which have fuelled many of the developments so far, will continue to drive forwards basic science and its applications. It will certainly be interesting to see what the next twist will be.

## References

- Allen, L., Beijersbergen, M. W., Spreeuw, R. J. C. & Woerdman, J. P. Orbital angular-momentum of light and the transformation of Laguerre–Gaussian laser modes. *Phys. Rev. A* **45**, 8185–8189 (1992).
- He, H., Friese, M., Heckenberg, N. R. & Rubinsztein-Dunlop, H. Direct observation of transfer of angular momentum to absorptive particles from a laser beam with a phase singularity. *Phys. Rev. Lett.* **75**, 826–829 (1995).
- Simpson, N., Dholakia, K., Allen, L. & Padgett, M. Mechanical equivalence of spin and orbital angular momentum of light: an optical spanner. *Opt. Lett.* **22**, 52–54 (1997).
- Poynting, J. The wave motion of a revolving shaft, and a suggestion as to the angular momentum in a beam of circularly polarised light. *Proc. R. Soc. Lond. A* **82**, 560–567 (1909).
- Beth, R. Mechanical detection and measurement of the angular momentum of light. *Phys. Rev.* **50**, 115–125 (1936).
- Jackson, J. *Classical Electrodynamics* 3rd edn (Wiley, 2007).
- Turnbull, G. A., Roberson, D. A., Smith, G. M., Allen, L. & Padgett, M. J. Generation of free-space Laguerre–Gaussian modes at millimetre-wave frequencies by use of a spiral phaseplate. *Opt. Commun.* **127**, 183–188 (1996).
- Beijersbergen, M. W., Allen, L., van der Veen, H. & Woerdman, J. P. Astigmatic laser mode converters and transfer of orbital angular momentum. *Opt. Commun.* **96**, 123–132 (1993).
- Bazhenov, V., Vasnetsov, M. V. & Soskin, M. S. Laser-beams with screw dislocations in their wave-fronts. *JETP Lett.* **52**, 429–431 (1990).
- Heckenberg, N. R., McDuff, R., Smith, C. P. & White, A. Generation of optical phase singularities by computer-generated holograms. *Opt. Lett.* **17**, 221–223 (1992).
- Guo, C., Liu, X., He, J. & Wang, H. Optimal annulus structures of optical vortices. *Opt. Express* **12**, 4625–4634 (2004).
- Nye, J. F. & Berry, M. Dislocations in wave trains. *Proc. R. Soc. Lond. A* **336**, 165–190 (1974).
- Berry, M., Nye, J. & Wright, F. The elliptic umbilic diffraction catastrophe. *Phil. Trans. R. Soc. Lond.* **291**, 453–484 (1979).
- Coullet, P., Gil, G. & Rocca, F. Optical vortices. *Opt. Commun.* **73**, 403–408 (1989).
- Wulff, K. *et al.* Aberration correction in holographic optical tweezers. *Opt. Express* **14**, 4169–4174 (2006).
- Jesacher, A. *et al.* Wavefront correction of spatial light modulators using an optical vortex image. *Opt. Express* **15**, 5801–5808 (2007).
- Ashkin, A., Dziedzic, J., Bjorkholm, J. & Chu, S. Observation of a single-beam gradient force optical trap for dielectric particles. *Opt. Lett.* **11**, 288–290 (1986).
- He, H., Heckenberg, N. R. & Rubinsztein-Dunlop, H. Optical particle trapping with higher-order doughnut beams produced using high efficiency computer generated holograms. *J. Mod. Opt.* **42**, 217–223 (1995).
- Friese, M., Enger, J., Rubinsztein-Dunlop, H. & Heckenberg, N. Optical angular-momentum transfer to trapped absorbing particles. *Phys. Rev. A* **54**, 1593–1596 (1996).
- Friese, M., Nieminen, T., Heckenberg, N. R. & Rubinsztein-Dunlop, H. Optical alignment and spinning of laser-trapped microscopic particles. *Nature* **394**, 348–350 (1998).
- Ashkin, A., Dziedzic, J. M. & Yamane, T. Optical trapping and manipulation of single cells using infrared laser beams. *Nature* **330**, 769–771 (1987).
- Sato, S., Ishigure, M. & Inaba, H. Optical trapping and rotational manipulation of microscopic particles and biological cells using higher-order mode Nd:YAG laser beams. *Electron. Lett.* **27**, 1831–1832 (1991).
- Paterson, L. *et al.* Controlled rotation of optically trapped microscopic particles. *Science* **292**, 912–914 (2001).
- MacDonald, M. *et al.* Revolving interference patterns for the rotation of optically trapped particles. *Opt. Commun.* **201**, 21–28 (2002).
- O’Neil, A. & Padgett, M. Rotational control within optical tweezers by use of a rotating aperture. *Opt. Lett.* **27**, 743–745 (2002).
- Kreysing, M. K. *et al.* The optical cell rotator. *Opt. Express* **16**, 16984–16992 (2008).
- Hoerner, F., Woerdemann, M., Mueller, S., Maier, B. & Denz, C. Full 3d translational and rotational optical control of multiple rod-shaped bacteria. *J. Biophoton.* **3**, 468–475 (2010).
- Higurashi, E., Sawada, R. & Ito, T. Optically induced angular alignment of trapped birefringent micro-objects by linearly polarized light. *Phys. Rev. E* **59**, 3676–3681 (1999).
- Galajda, P. & Ormos, P. Orientation of flat particles in optical tweezers by linearly polarized light. *Opt. Express* **11**, 446–451 (2003).
- Higurashi, E., Ukita, H., Tanaka, H. & Ohguchi, O. Optically induced rotation of anisotropic micro-objects fabricated by surface micromachining. *Appl. Phys. Lett.* **64**, 2209–2210 (1994).
- Higurashi, E., Ohguchi, O., Tamamura, T., Ukita, H. & Sawada, R. Optically induced rotation of dissymmetrically shaped fluorinated polyimide micro-objects in optical traps. *J. Appl. Phys.* **82**, 2773–2779 (1997).
- Galajda, P. & Ormos, P. Complex micromachines produced and driven by light. *Appl. Phys. Lett.* **78**, 249–251 (2001).
- Galajda, P. & Ormos, P. Rotors produced and driven in laser tweezers with reversed direction of rotation. *Appl. Phys. Lett.* **80**, 4653–4655 (2002).
- Knöner, G. *et al.* Integrated optomechanical microelements. *Opt. Express* **15**, 5521–5530 (2007).
- Higurashi, E., Sawada, R. & Ito, T. Optically induced rotation of a trapped micro-object about an axis perpendicular to the laser beam axis. *Appl. Phys. Lett.* **72**, 2951–2953 (1998).
- Dienerowitz, M., Mazilu, M., Reece, P., Krauss, T. & Dholakia, K. Optical vortex trap for resonant confinement of metal nanoparticles. *Opt. Express* **16**, 4991–4999 (2008).
- Ashkin, A. Forces of a single-beam gradient laser trap on a dielectric sphere in the ray optics regime. *Biophys. J.* **61**, 569–582 (1992).
- O’Neil, A. & Padgett, M. Axial and lateral trapping efficiency of Laguerre–Gaussian modes in inverted optical tweezers. *Opt. Commun.* **193**, 45–50 (2001).
- Bowman, R., Gibson, G. & Padgett, M. Particle tracking stereomicroscopy in optical tweezers: control of trap shape. *Opt. Express* **18**, 11785–11790 (2010).
- Gahagan, K. & Swartzlander, G. A. Optical vortex trapping of particles. *Opt. Lett.* **21**, 827–829 (1996).
- Prentice, P. *et al.* Manipulation and filtration of low index particles with holographic Laguerre–Gaussian optical trap arrays. *Opt. Express* **12**, 593–600 (2004).
- Lorenz, R. *et al.* Vortex-trap-induced fusion of femtoliter-volume aqueous droplets. *Anal. Chem.* **79**, 224–228 (2007).
- O’Neil, A., MacVicar, I., Allen, L. & Padgett, M. Intrinsic and extrinsic nature of the orbital angular momentum of a light beam. *Phys. Rev. Lett.* **88**, 053601 (2002).
- Garces-Chavez, V. *et al.* Observation of the transfer of the local angular momentum density of a multiringed light beam to an optically trapped particle. *Phys. Rev. Lett.* **91**, 093602 (2003).
- Curtis, J. & Grier, D. Structure of optical vortices. *Phys. Rev. Lett.* **90**, 133901 (2003).
- Jesacher, A., Fühapter, S., Maurer, C., Bernet, S. & Ritsch-Marte, M. Holographic optical tweezers for object manipulations at an air–liquid surface. *Opt. Express* **14**, 6342–6352 (2006).
- Leach, J. & Padgett, M. Observation of chromatic effects near a white-light vortex. *New J. Phys.* **5**, 154 (2003).

48. Mariyenko, I., Strohaber, J. & Uiterwaal, C. Creation of optical vortices in femtosecond pulses. *Opt. Express* **13**, 7599–7608 (2005).
49. Sztul, H., Kartazayev, V. & Alfano, R. Laguerre–Gaussian supercontinuum. *Opt. Lett.* **31**, 2725–2727 (2006).
50. Wright, A., Girkin, J., Gibson, G., Leach, J. & Padgett, M. Transfer of orbital angular momentum from a super-continuum, white-light beam. *Opt. Express* **16**, 9495–9500 (2008).
51. Tao, S., Yuan, X., Lin, J., Peng, X. & Niu, H. Fractional optical vortex beam induced rotation of particles. *Optics Express* **13**, 7726–7731 (2005).
52. Courtial, J. & Padgett, M. Limit to the orbital angular momentum per unit energy in a light beam that can be focussed onto a small particle. *Opt. Commun.* **173**, 269–274 (2000).
53. Hayasaki, Y., Itoh, M., Yatagai, T. & Nisida, N. Nonmechanical optical manipulation of microparticle using spatial light modulator. *Opt. Rev.* **6**, 24–27 (1999).
54. Reicherter, M., Haist, T., Wagemann, E. & Tiziani, H. Optical particle trapping with computer-generated holograms written on a liquid-crystal display. *Opt. Lett.* **24**, 608–610 (1999).
55. Liesener, J., Reicherter, M., Haist, T. & Tiziani, H. Multi-functional optical tweezers using computer-generated holograms. *Opt. Commun.* **185**, 77–82 (2000).
56. Curtis, J., Koss, B. & Grier, D. Dynamic holographic optical tweezers. *Opt. Commun.* **207**, 169–175 (2002).
57. Grier, D. A revolution in optical manipulation. *Nature* **424**, 810–816 (2003).
58. Curtis, J. & Grier, D. Modulated optical vortices. *Opt. Lett.* **28**, 872–874 (2003).
59. Eriksen, R., Rodrigo, P., Daria, V. & Gluckstad, J. Spatial light modulator-controlled alignment and spinning of birefringent particles optically trapped in an array. *Appl. Opt.* **42**, 5107–5111 (2003).
60. Preece, D. *et al.* Independent polarisation control of multiple optical traps. *Opt. Express* **16**, 15897–15902 (2008).
61. Roichman, Y., Grier, D. & Zaslavsky, G. Anomalous collective dynamics in optically driven colloidal rings. *Phys. Rev. E* **75**, 020401 (2007).
62. Ladavac, K. & Grier, D. Colloidal hydrodynamic coupling in concentric optical vortices. *Europhys. Lett.* **70**, 548–554 (2005).
63. Lee, S.-H. & Grier, D. Giant colloidal diffusivity on corrugated optical vortices. *Phys. Rev. Lett.* **96**, 190601 (2006).
64. Ladavac, K. & Grier, D. Microoptomechanical pumps assembled and driven by holographic optical vortex arrays. *Opt. Express* **12**, 1144–1149 (2004).
65. Pralle, A., Florin, E., Stelzer, E. & Horber, J. Local viscosity probed by photonic force microscopy. *Appl. Phys. A* **66**, S71–S73 (1998).
66. Bishop, A., Nieminen, T., Heckenberg, N. & Rubinshtein-Dunlop, H. Optical microrheology using rotating laser-trapped particles. *Phys. Rev. Lett.* **92**, 198104 (2004).
67. Parkin, S. *et al.* Highly birefringent vaterite microspheres: production, characterization and applications for optical micromanipulation. *Opt. Express* **17**, 21944–21955 (2009).
68. Vogel, R. *et al.* Synthesis and surface modification of birefringent vaterite microspheres. *Langmuir* **25**, 11672–11679 (2009).
69. Parkin, S. J., Knöner, G., Nieminen, T. A., Heckenberg, N. R. & Rubinshtein-Dunlop, H. Picoliter viscometry using optically rotated particles. *Phys. Rev. E* **76**, 041507 (2007).
70. Leach, J. *et al.* Comparison of Faxen's correction for a microsphere translating or rotating near a surface. *Phys. Rev. E* **79**, 026301 (2009).
71. Leach, J., Mushfique, H., di Leonardo, R., Padgett, M. & Cooper, J. An optically driven pump for microfluidics. *Lab. Chip.* **6**, 735–739 (2006).
72. Jesacher, A., Maurer, C., Schwaighofer, A., Bernet, S. & Ritsch-Marte, M. Full phase and amplitude control of holographic optical tweezers with high efficiency. *Opt. Express* **16**, 4479–4486 (2008).
73. Roichman, Y., Sun, B., Roichman, Y., Amato-Grill, J. & Grier, D. Optical forces arising from phase gradients. *Phys. Rev. Lett.* **100**, 013602 (2008).
74. Lee, S., Roichman, Y. & Grier, D. Optical solenoid beams. *Opt. Express* **18**, 6988–6993 (2010).
75. Baumgartl, J., Mazilu, M. & Dholakia, K. Optically mediated particle clearing using airy wavepackets. *Nature Photon.* **2**, 675–678 (2008).
76. Daria, V. R., Palima, D. Z. & Gluckstad, J. Optical twists in phase and amplitude. *Opt. Express* **19**, 476–481 (2011).
77. Asavei, T., Loke, V. L. Y., Nieminen, T. A., Heckenberg, N. R. & Rubinshtein-Dunlop, H. Optical paddle-wheel. *Proc. SPIE* **7400**, 740020 (2009).
78. Lewittes, M., Arnold, S. & Oster, G. Radiometric levitation of micron sized spheres. *Appl. Phys. Lett.* **40**, 455–457 (1982).
79. Shvedov, V., Desyatnikov, A., Rode, A., Krolkowski, W. & Kivshar, Y. Optical guiding of absorbing nanoclusters in air. *Opt. Express* **17**, 5743–5757 (2009).
80. Shvedov, V. *et al.* Giant optical manipulation. *Phys. Rev. Lett.* **105**, 118103 (2010).
81. Shvedov, V. *et al.* Selective trapping of multiple particles by volume speckle field. *Opt. Express* **18**, 3137–3142 (2010).
82. O'Holleran, K., Dennis, M. R., Flossmann, F. & Padgett, M. J. Fractality of light's darkness. *Phys. Rev. Lett.* **100**, 053902 (2008).
83. Furlapter, S., Jesacher, A., Bernet, S. & Ritsch-Marte, M. Spiral phase contrast imaging in microscopy. *Opt. Express* **13**, 689–694 (2005).
84. Swartzlander, G. *et al.* Astronomical demonstration of an optical vortex coronagraph. *Opt. Express* **16**, 10200–10207 (2008).
85. Dholakia, K., Simpson, N., Padgett, M. & Allen, L. Second-harmonic generation and the orbital angular momentum of light. *Phys. Rev. A* **54**, R3742–R3745 (1996).
86. Mair, A., Vaziri, A., Weihs, G. & Zeilinger, A. Entanglement of the orbital angular momentum states of photons. *Nature* **412**, 313–316 (2001).
87. Gibson, G. *et al.* Free-space information transfer using light beams carrying orbital angular momentum. *Opt. Express* **12**, 5448–5456 (2004).
88. Thidé, B. *et al.* Utilization of photon orbital angular momentum in the low-frequency radio domain. *Phys. Rev. Lett.* **99**, 087701 (2007).

## Acknowledgements

M.J.P. acknowledges financial support from the Royal Society. Figures 2–4 were produced with TIM, a custom Java raytracer (<http://arxiv.org/abs/1101.3861v1>).